AGU PUBLICATIONS

Geophysical Research Letters

RESEARCH LETTER
10.1002/2016GL072486

Key Points:
- Homogeneous freezing events in cirrus are highly transient and localized
- Strong diffusion and turbulence affects the number of nucleated ice crystals
- Modeling homogeneous freezing requires high temporal and spatial resolution

Supporting Information:
- Supporting Information S1
- Figure S1
- Figure S2

Correspondence to:
B. Kärcher,
bernd.kaercher@dlr.de

Citation:
Kärcher, B. and E. J. Jensen (2017), Microscale characteristics of homogeneous freezing events in cirrus clouds, *Geophys. Res. Lett.*, *44*, doi:10.1002/2016GL072486.

Received 30 DEC 2016
Accepted 2 FEB 2017
Accepted article online 4 FEB 2017

Microscale characteristics of homogeneous freezing events in cirrus clouds

B. Kärcher[1] **and E. J. Jensen**[2]

[1]Deutsches Zentrum für Luft- und Raumfahrt, Institut für Physik der Atmosphäre, Wessling, Germany, [2]National Aeronautics and Space Administration, Ames Research Center, Moffett Field, California, USA

Abstract We investigate homogeneous freezing of aqueous aerosol particles, a fundamental ice formation process in cirrus clouds. We estimate freezing time scales and vertical extensions of freezing layers, demonstrating that such freezing events are highly transient and localized. While time scales decrease with increasing vertical velocity driving ice nucleation, layer depths are weak functions of the vertical velocity. Our results are used to discuss possible effects of turbulent diffusion and entrainment-mixing on homogeneous freezing in cirrus. Large turbulent diffusivity acts to broaden water vapor-depleted freezing layers and facilitate sedimentation of freshly nucleated ice crystals out of them into ice-supersaturated air. Homogeneous freezing events could be affected by microscale turbulence in episodes of intense turbulence dissipation rates, although such episodes are rare. We conjecture that freezing layers are broader in the case of heterogeneous ice nucleation and effects of sedimentation on nucleation increase in importance. Our findings point to the difficulty of inferring nucleated cirrus ice crystal numbers from measurements and place tight constraints on cirrus models with regard to spatial and temporal resolution.

1. Introduction

Uncertainties in assessing the anthropogenic impact on cirrus clouds and estimating their role in a future climate are caused in part by incomplete understanding of ice formation mechanisms [*Kärcher*, 2017]. In particular, research studies have difficulties in reconciling observed ice crystal number densities in upper tropospheric cirrus with results from models [e.g., *Jensen et al.*, 2016a]. Depending on temperature and relative humidity, the liquid-to-ice phase transition in cirrus is induced in supercooled aqueous aerosol particles and water droplets.

The roles of aerosol particles in cirrus ice formation, especially the role of heterogeneous ice nuclei (IN), can only be assessed with confidence if characteristics of small-scale dynamical forcing of ice nucleation and basic features of the most fundamental ice nucleation process—homogeneous freezing of supercooled liquid water—are well understood. While some progress was recently made in quantifying mesoscale variability in vertical wind velocities as a key driver of ice nucleation [*Dinh et al.*, 2016; *Jensen et al.*, 2016b; *Shi and Liu*, 2016], microscale characteristics of homogeneous aerosol freezing events have not yet been scrutinized.

The present study makes a first attempt to explore characteristics of homogeneous freezing events across the wide range of temperatures where cirrus clouds form. This includes the cold (temperatures $T \simeq 180-205$ K) tropical tropopause layer (TTL)—the region in the tropical upper troposphere above the mean level of deep convective outflow and below the tropopause—and the warm cirrus regime ($T \simeq 230-240$ K). *Kärcher and Seifert* [2016] analyzed the glaciation process in high-reaching liquid water clouds due to homogeneous droplet freezing in the warm cirrus regime. Here we investigate the temporal and spatial scales over which homogeneous aqueous aerosol freezing events unfold at colder temperatures.

To begin with, we delineate a homogeneous freezing event as a baseline case by means of a spectral air parcel simulation in section 2. We continue investigating the physical characteristics of these events analytically in section 3. The quantitative information made available in this way allows us to discuss in section 4 for the first time potential effects of turbulent diffusion and entrainment mixing on homogeneous freezing in cirrus. Our results lend themselves to repercussions with regard to properties of IN-induced nucleation layers as well as to modeling homogeneous freezing events and detecting them in airborne measurements, as summarized in section 5. The paper concludes with a brief summary of our main findings in section 6.

2. Freezing Relaxation

Homogeneous freezing conditions in adiabatic air parcels are brought about by cooling of air. We study homogeneous freezing events in an air parcel framework [*Kärcher*, 2003]. Air parcels — lifted at a constant upward vertical wind velocity ($w > 0$) along the dry adiabatic lapse rate ($\Gamma = -9.8$ K/km) — experience cooling rates $\dot{T} = w\Gamma$. Times are converted to altitudes, z (relative to an initial altitude of the rising air parcel), via $z = wt$.

The amount of water molecules to be exchanged between the vapor and the liquid to equilibrate sub-μm aerosol particles is small, and the time for this exchange is very short. This means that the water activity in aerosol particles approximately equals to the liquid water saturation ratio of the ambient gas phase, $a_w = S_w(T)$. The latter is related to the ice saturation ratio via $S_i = S_w\eta$, where $\eta(T)$ is the ratio of liquid water and ice saturation vapor pressures. Homogeneous freezing occurs at large ice supersaturation ($S_i - 1 > 0.45$).

To investigate the homogeneous freezing process in upper tropospheric solution particles, we make use of the activity-based freezing rate coefficient, $J(a_w, T)$, per unit droplet volume per unit time [*Koop et al.*, 2000]. It depends on T and on the water activity of the solution particles, a_w. The latent heat released in freezing sub-μm aerosol particles is very small, and its transport is rapid, so we make no distinction between air and liquid-phase temperatures. The ice crystal production rate (per unit time) due to freezing follows from $j = V J$, with the mean liquid water volume, V, per particle.

Freezing of water-containing particles and depositional growth of ice crystals nucleating from them control the evolution of the three water phases during ice formation. The self-limiting nature of freezing events is encapsulated in the freezing relaxation concept underlying our analysis. This framework has been applied to estimate nucleated ice crystal properties due to homogeneous freezing of aqueous aerosol particles [*Kärcher and Lohmann*, 2002] and cloud water droplets [*Kärcher and Seifert*, 2016].

In essence, freezing relaxation states that ice nucleation terminates when the growth of already nucleated ice crystals ("freezing") begins to drive the ice supersaturation, $S_i - 1$, and thus the nucleation rates of yet unfrozen droplets to zero ("relaxation"). The point in time where the freezing pulse, j, defined as the number of ice crystals nucleating per unit time, takes its maximum is denoted by $t_\star$. Freezing relaxation occurs close to $t_\star$. We assume that $j(t)$ takes an exponential form prior to $t_\star$, $j\left(t \le t_\star\right) = j_{\max} \exp\left[-|t - t_\star|/\tau_n\right]$, where τ_n is the characteristic nucleation time scale and $j\left(t > t_\star\right) = 0$.

To illustrate freezing relaxation for TTL conditions, Figures 1a and 1b show the evolution of $j/j_{\max}$ and S_i, from a numerical parcel simulation. The distance over which an air parcel needs to be lifted from the frost point to reach homogeneous freezing conditions amounts to a few hundred meters. The time step used in the simulation was 0.2 s, resolving 0.1 m at $w = 0.5$ m/s. This value of w is well in the range of gravity wave-induced values in the upper troposphere [*Hoyle et al.*, 2005] including the TTL [*Podglajen et al.*, 2016].

Due to the very strong water activity dependence of the homogeneous aerosol freezing rate coefficient, j rises very sharply only when S_i surpasses a threshold, ≈ 1.63. This contrasts homogeneous freezing for pure liquid water droplets, where the rate coefficient only depends on temperature, making the freezing pulse broader [*Kärcher and Seifert*, 2016] (although still narrow on the altitude scale shown in Figure 1a).

A comparison of the numerical result with the assumed exponential evolution of j near its peak (at $z_\star$) is given in Figure 1c. The simulated pulse (solid curve) is not perfectly exponential for $z \le z_\star$. The rate of decay of $j(z > z_\star)$ depends on the liquid water volume in aerosols but typically to a much larger degree on the total number and mean size of the already nucleated ice crystals. The faster the updraft, the more ice crystals form and the faster the pulse tails off. The freezing relaxation approximation (dashed curve) therefore underestimates the total width of j. Nonetheless, we employ a one-sided exponential pulse since this leads to a succinct description of freezing layer depths. A potential underestimation of layer depths and associated freezing time scales following from the exponential approximation is accounted for by introducing an empirical parameter constrained by the numerical simulation.

3. Freezing Time Scale and Layer Depth

Based on an exponential increase of the freezing pulse, the characteristic time scale of homogeneous freezing events is defined by

$$\frac{1}{\tau_n} \equiv \frac{\mathrm{d}\ln(j)}{\mathrm{d}t} = \frac{\mathrm{d}\ln(j)}{\mathrm{d}T}\dot{T} \simeq \frac{\mathrm{d}\ln(J)}{\mathrm{d}T}\dot{T}\,; \tag{1}$$

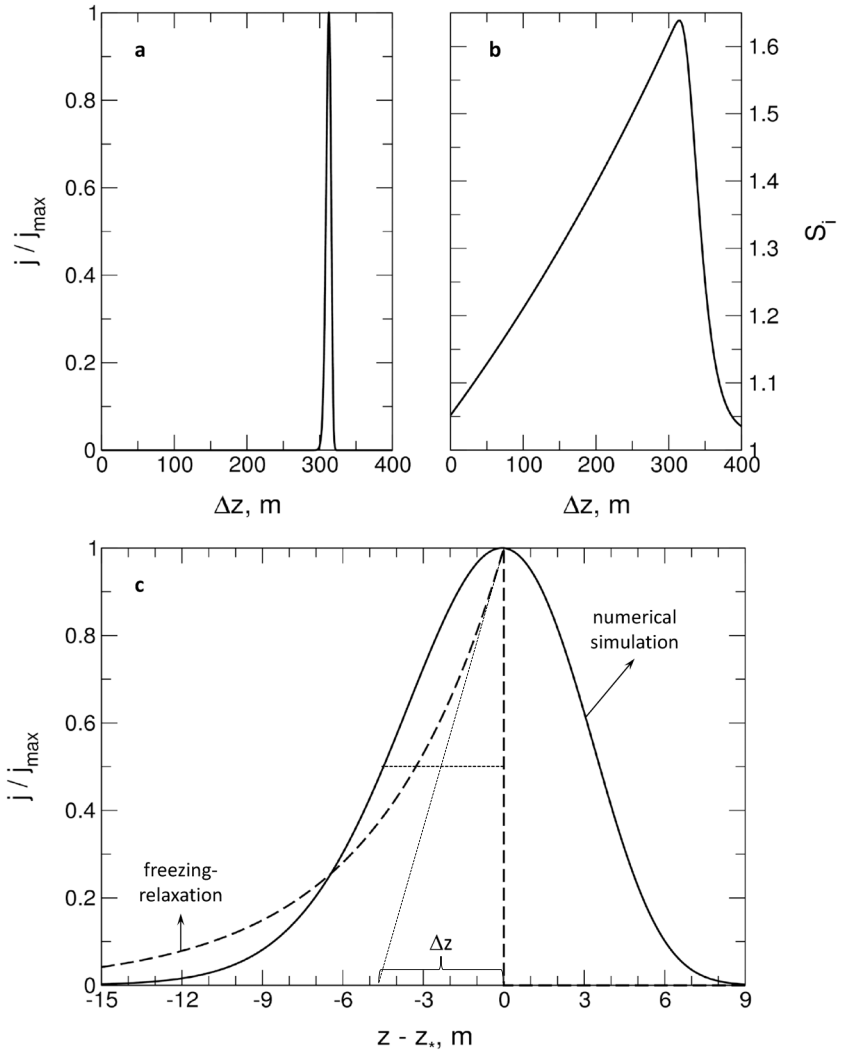

Figure 1. Evolution of (a) the normalized freezing pulse—the ice crystal formation rate due to homogeneous aerosol freezing—and (b) the ice saturation ratio from a numerical parcel simulation of ice nucleation and growth using a constant updraft speed, $w = 0.5$ m/s, and starting near ice saturation. (c) Zoom of j/j_{max} around the peak region (solid curve) and an exponential fit (dashed curve) underlying the freezing relaxation concept, using the scaling depth $\Delta z = 4.8$ m. The conditions at $z = z_\star = 313$ m, where j takes its maximum, correspond to $T_\star \approx 192$ K and $S_{i\star} \approx 1.63$ which are almost constant across the distance Δz centered around the peak.

the latter approximation holds, since the relative change of the liquid water volume is much smaller than that of the freezing rate coefficient. The total rate of change of $\ln(J)$ [*Koop et al.*, 2000] with respect to a unit change in T follows from

$$\frac{1}{\delta T} \equiv \frac{\mathrm{d}\ln(J)}{\mathrm{d}T} = \frac{\partial \ln(J)}{\partial a_w}\Big|_T \frac{\mathrm{d}a_w}{\mathrm{d}T} + \frac{\partial \ln(J)}{\partial T}\Big|_{a_w}. \tag{2}$$

We apply the Clausius-Clapeyron relationship, $\mathrm{d}S_w/\mathrm{d}T = -S_w L/\left(R_w T^2\right)$, to evaluate the activity derivative, $\mathrm{d}a_w/\mathrm{d}T$, where $L(T)$ is the latent heat of sublimation [*Murphy and Koop*, 2005] and R_w is the gas constant for water vapor. The first term in equation (2) exceeds the second by more than an order of magnitude and is therefore more important in determining τ_n. (The first term vanishes for freezing of pure water droplets, in which case $a_w = 1$.) For super-μm aerosol particles at sufficiently high cooling rates, a_w may lag behind its equilibrium counterpart, S_w [*Haag et al.*, 2003]. However, the number concentration of such large particles is very small, and homogeneous ice nucleation will cause much smaller aerosol particles to freeze at common mesoscale updraft speeds.

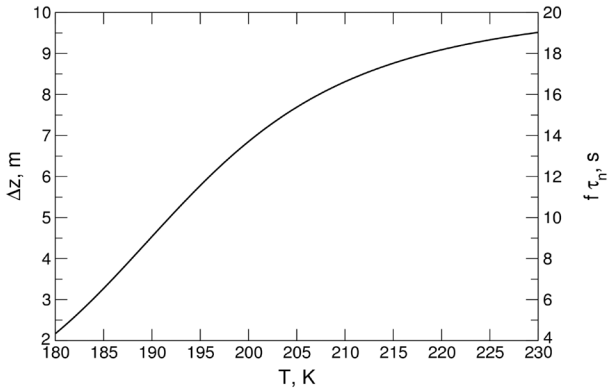

Figure 2. Depth of homogeneous freezing layers obtained from equation (4) for $w = 0.5$ m/s and corresponding effective nucleation time scales, $f\tau_n = \Delta z/w$, versus temperature. Layers are shallower and freezing times shorter for lower T, since the freezing rate coefficient increases more steeply upon lowering T owing to its strong dependence on T via the water activity.

In equations (1) and (2), T and S_w (or equivalently S_i) are not known, so we seek a relationship that allows us to determine their values close to the maximum of the freezing pulse. We can estimate those variables from $\int VJdt = q$, using $J \propto \exp(-T(t)/\delta T)$ and liquid water volume, V; cooling rate, $\dot{T}$; and frozen aerosol particle fraction, q. The integral can be solved in closed form for constant $V, \dot{T}$, and δT, leading to freezing relaxation temperatures, $T_\star$, that decrease in proportion to $\ln(w)$ in the case of homogeneous water droplet freezing [see *Kärcher and Seifert*, 2016, Figure 5b]. For aqueous aerosol particles, δT depends on T (see equations (1) and (2)); for simplicity, we evaluate the integral approximately by iterating the equation

$$V J\left(a_w, T\right)\ \tau_n\left(T, \dot{T}\right) = q \implies T_\star\,, \tag{3}$$

with $V = 0.065\mu m^3$, corresponding to a mean aerosol particle radius of 0.25μm, and with the upper limit value $q = 1$ (in nature, $q = q(\dot{T})$). The solution $\{T_\star, S_{i\star} \equiv S_i(T_\star)\}$ — approximating the conditions at the freezing peak — depends only weakly on V, $\dot{T}$, and q, because J depends strongly on T.

The depth of the freezing layer, Δz, follows from combining equations (1) and (2), evaluated at conditions from equation (3):

$$\Delta z = w \cdot f\tau_n. \tag{4}$$

Introducing the empirical parameter $f \geq 1$ defines an effective freezing time scale, $f\tau_n = \Delta z/w$, and corrects for the use of an approximate exponential freezing pulse. Setting $f = 1$ yields an uncorrected layer depth $\Delta z = 1.35$ m for the conditions in Figure 1. The time scale inferred from an exponential pulse better fits the numerical simulation result when using $f = 3.5$ (Figure 1c), in which case Δz is equal to the width of the simulated pulse at half maximum (≈ 5 m; horizontal dotted line).

Equation (4) will be used to evaluate diffusion, mixing, and sedimentation time scales. According to equation (1), $\tau_n \propto 1/w$; hence, in stronger updrafts air parcels reach higher levels at a faster rate, but at the same time freezing within the pulse proceeds more rapidly. Both effects cancel, so Δz from equation (4) does not depend explicitly on $\dot{T}$ (or w); a weak implicit dependence remains via the dependence of $T_\star$, hence, δT, on w. For instance, at $T = 190$ K upon decreasing (increasing) w by a factor of 10, Δz increases (decreases) by less than 5 %.

Capturing all freezing particles along the entire evolution of j results in longer time scales (broader layers) than focussing on freezing of particles around the peak region of j, as done here. First-to-last time scales for TTL homogeneous freezing events simulated across a wide range of updraft speeds and environmental conditions are ≈ 1 min [*Jensen et al.*, 2016b; *Dinh et al.*, 2016]. In the example discussed in Figure 1, the width encompassing the whole freezing pulse is ≈ 24 m, corresponding to a time duration of 0.8 min.

Figure 2 confirms the numerical result that, relative to the lifting distance, homogeneous freezing layers are very shallow. The shallowness is caused by the steep gradient of J with temperature (the smallness of $|\delta T|$), resulting mainly from the very steep, explicit dependence on a_w — the freezing pulse is therefore confined to a very narrow region around its peak. Layers are thicker in the case of homogeneous freezing of water droplets, because the associated rate coefficient [*Riechers et al.*, 2013] is not constrained by water activity as $(\partial \ln(J)/\partial a_w)_T = 0$ and $|\delta T| \simeq 0.28$ K at $T \approx 235$ K is about tenfold larger than values for aqueous aerosol particles taken from equation (2) for $T > 230$ K. This leads to an uncorrected layer depth of about 30 m for water droplet freezing [*Kärcher and Seifert*, 2016].

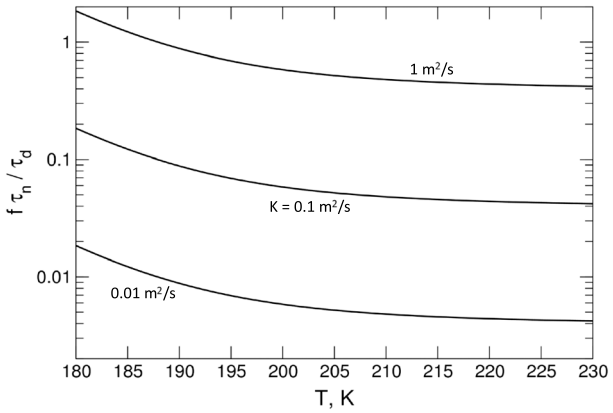

Figure 3. Ratio of homogeneous freezing and turbulent diffusion time scales versus temperature shown for $w = 0.5$ m/s and selected values for the vertical diffusion coefficient (see text).

Freezing layers might be viewed as an aspect of cirrus cloud morphology—one that evolves rapidly with time due to subsequent physical processes such as ice crystal sedimentation, turbulence, and wind shear. The freezing layer depth is not necessarily related to the depth of observed cirrus layers. In the TTL, cirrus layers with depths 2–500 m have been observed containing high ice number concentrations most likely formed by homogeneous freezing [*Jensen et al.*, 2013a]. Thin cloud layers can also be produced by rapid, local cooling due to small-scale gravity waves. The thickness of such layers may be controlled by the vertical profile of supersaturation and, over time, subsequent effects of sedimentation and diffusion.

4. Diffusion, Mixing, and Sedimentation

The shallowness of homogeneous freezing layers raises questions whether (i) turbulent diffusion broadens freezing layers; (ii) the nucleation process is affected by entrainment and mixing; and (iii) ice crystals fall out of the layer during nucleation.

Turbulent diffusion. Fully developed turbulence is rare in the upper troposphere. The approximate concept of turbulent diffusion describes the average outcome of a suite of processes associated with turbulence. Knowledge of associated diffusion coefficients, K, is poor, and estimates of their values are uncertain. Generally, large K values are associated with intermittent, brief episodes of strong turbulence often related to high wind shear and weak thermal stability. Aircraft measurements hint at average values for the vertical diffusivity in the range 0.01–0.1 m^2/s in the TTL (A. Podglajen et al., Small-scale wind fluctuations in the tropical tropopause layer from aircraft measurements: Occurrence, nature and impact on vertical mixing, submitted manuscript, 2017). While most values are below this range, peak local values can be orders of magnitude larger. In the midlatitude upper troposphere, a range $K = 0.1$–4 m^2/s has been inferred from observations depending on wind shear [*Dürbeck and Gerz*, 1996]. The time scale associated with turbulent diffusion is given by $\tau_d = (\Delta z)^2/(2K)$. This time scale is a measure of how quickly turbulence acts to spread the layer (or to disperse tracers contained in it).

Figure 3 shows the ratio $f\tau_n/\tau_d = 2K/(w\Delta z)$ versus T for a range of diffusivities and Δz values taken from Figure 2 and $w = 0.5$ m/s. If $f\tau_n < \tau_d$, nucleation occurs too rapidly to be affected by turbulent diffusion. However, diffusion subsequently dilutes nucleated ice number concentrations (per unit volume of air) with time, t, well after the freezing event. Diffusion also enhances the growth and hence sedimentation rates of freshly nucleated ice crystals by replenishing water vapor within the freezing layer. Conversely, if $f\tau_n > \tau_d$, diffusion is rapid enough to impact the freezing process itself by diluting water vapor (and heat) within the air parcel. For the present choice of w, this regime is hardly ever realized.

Entrainment mixing. Turbulence acts to break large-scale flow structures down to the molecular level, where ice nucleation ultimately takes place. This breakdown of large-scale structures is caused by convective stirring enhancing spatial gradients in the flow field and by molecular diffusion. In fully developed inertial range turbulence, a characteristic scale measuring the time it takes for turbulent eddies of size Δz to be reduced to the dissipation length scale is $\tau_{\Delta z} = [(\Delta z)^2/\epsilon]^{1/3}$, with the energy dissipation rate per unit mass of air, ϵ.

The ratio $\mathrm{Da}_n = f\tau_n/\tau_{\Delta z}$ defines a Damköhler number for homogeneous aerosol freezing. If $\mathrm{Da}_n > 1$, then entrainment mixing affects homogeneous freezing. Values of ϵ satisfying this criterion are $\epsilon > w^3/\Delta z$, or $\epsilon > 0.01$ m^2/s^3 for $w = 0.5$ m/s and Δz values from Figure 2. For water droplets freezing in the warm cirrus regime, especially in outflow regions of deep convective clouds, the criterion is less restrictive, $\epsilon > 0.004$ m^2/s^3, as freezing layers are thicker. However, cold convective cloud outflow regions may exhibit larger updraft speeds than those measured in the stable upper troposphere. Measurements show high ϵ values 0.01–0.1 m^2/s^3 in

the TTL [*Podglajen et al.*, 2016] and the high-latitude upper troposphere [*Li et al.*, 2016], representing the tail of probability distributions. This means that homogeneous freezing can be affected by entrainment mixing during episodes of intense but rare microscale turbulence.

In the warm cirrus regime, entrainment mixing may even be efficient enough to evaporate cloud water droplets before they freeze homogeneously. The droplet evaporation time scale, τ_e, derived and discussed in the supporting information, defines a Damköhler number related to this process, $\mathrm{Da}_e = \tau_e / \tau_{\Delta z}$. For $\tau_e > 10$ s and $\Delta z = 30$ m, the requirement $\mathrm{Da}_e > 1$ implies that $\epsilon > 1\ \mathrm{m}^2/\mathrm{s}^3$. Such high levels of turbulence intensity may seldom be realized [*Lane and Sharman*, 2014].

Sedimentation. Homogeneous freezing self-terminates before freshly nucleated ice crystals sediment out of the nucleation layer; a derivation of sedimentation rates based on mean sizes of ice crystals at the point of homogeneous freezing relaxation according to [*Kärcher and Lohmann*, 2002] is given in the supporting information. Furthermore, for the duration of the freezing pulse, sedimentation cannot compete with turbulent diffusion except in regions with low turbulent diffusivity (Figure S1 in the supporting information). Juxtaposing the relative roles of sedimentation and diffusion reveals two further implications for processes occurring immediately after the homogeneous freezing event.

If nucleation layers contain only a few ice crystals (the exact number depending on w and the possible presence of IN), supersaturation in those layers can stay high for a long time, ice crystals grow large, and sediment rapidly [*Jensen et al.*, 2008; *Kärcher et al.*, 2014; *Murphy*, 2014]. A few ice crystals can result from pure homogeneous freezing either in sustained, weak updrafts, or, more likely, when air parcel trajectories are exposed to variability in temporal updraft speeds, i.e., arising from a spectrum of gravity waves.

According to observed frequency statistics of small-scale vertical wind velocities [*Jensen et al.*, 2013b, 2016b; *Podglajen et al.*, 2016; *Dinh et al.*, 2016], layers with high ice crystal number concentrations ($>0.1\ \mathrm{cm}^{-3}$) form occasionally. In those layers, the initial, high supersaturation is rapidly quenched and ice crystals stay small making sedimentation ineffective. Diffusion causes ice crystals to spread out of the layer and become exposed to ambient ice-supersaturated air, enabling further growth and enhancing sedimentation.

5. Implications

Heterogeneous ice nuclei. At cirrus altitudes, IN number concentrations are orders of magnitude smaller than those of aqueous particles. This means that in cases with high cooling rates, ice crystals nucleating on IN attain larger mean sizes during the nucleation event relative to those generated by homogeneous freezing at similar cooling rates. Moreover, nucleation times scales for IN are longer when heterogeneous nucleation occurs over a wider range of supersaturation (leading to shallower gradients of IN rate coefficients with temperature), implying wider nucleation layer depths. As a result, sedimentation becomes relatively more important than diffusion compared to homogeneous freezing.

Measurements of nucleated ice crystal numbers. Homogeneous freezing zones are highly localized and transient, minimizing chances to probe those zones with research aircraft [*Diao et al.*, 2013; *Dinh et al.*, 2014]. Satellite observations lack spatial and temporal resolution to capture those zones. Furthermore, sedimentation and turbulent diffusion dilute ice number concentrations after formation, leading to ice concentrations measured in situ that are lower than those predicted by parcel nucleation simulations. Drawing conclusions from aircraft data regarding ice formation mechanisms is therefore problematic, especially if microphysical data are not complemented by ancillary information on whether cirrus ice crystals formed in situ in the first place.

Cirrus cloud modeling. The shallowness of homogeneous freezing layers places tight constraints on the spatial and temporal resolution of cirrus models. Our results conform with earlier findings that ≈ 1 m vertical resolution is required for realistic simulation of homogeneous freezing in cirrus in models where ice cloud properties are discretized over a fixed grid [e.g., *Lin et al.*, 2005]. We emphasize that high temporal resolution is also needed and suggest to use time steps in nucleation models, $\delta t = \delta z / w$, that resolve vertical distances $\delta z < 1$ m. This implies subsecond time steps for simulations driven by mesoscale gravity waves. Using coarse vertical resolution and long time steps in representing homogeneous freezing events in computer simulations likely overestimates the number of nucleated ice crystals per event and may cause numerical artifacts. This misrepresentation of homogeneous freezing affects the prediction of cirrus cloud development.

Homogeneous freezing must be parameterized in cloud-resolving models, and perhaps even in large-eddy simulations, which are typically employed with vertical resolutions on the order of 10–100 m. Modeling cirrus

formation with confidence requires at least a one-dimensional framework in order to include effects of turbulent diffusion and sedimentation for meaningful comparisons with observations. Moreover, all scales down to the dissipation length scale need to be resolved to capture effects of turbulent stirring and molecular diffusion on homogeneous ice formation processes. For IN, the resolution requirements may be relaxed due to longer nucleation time scales and correspondingly thicker nucleation layers.

6. Summary

We have shown that homogeneous freezing of supercooled aerosol particles occurs on short time scales (seconds) and small vertical scales (meters). These scales tend to increase with temperature, and the spatial scale is only weakly dependent on the updraft speed. Over the duration of a homogeneous freezing event, ice crystals do not sediment out of the freezing layer.

The effect of turbulent diffusion is to dilute homogeneously nucleated ice crystal number concentrations in regions with high vertical diffusivity. Moreover, as freezing layers are embedded in highly ice-supersaturated air, turbulent diffusion tends to increase the efficiency of sedimentation by enhancing the supersaturation in vapor-depleted freezing layers leading to additional water uptake and thereby increased ice crystal fall speeds. At the same time, diffusion transports freshly nucleated ice crystals out of the layers.

We have used cooling rates that are constant during a freezing event. In nature, the combined effects of freezing, diffusion, and sedimentation on the distribution of cloud ice after a freezing event depend on temporal evolution of small-scale cooling rates (rapid temperature fluctuations) along air parcel trajectories and on vertical profiles of ice supersaturation. Numerical models required to simulate and further study those effects needed to employ very fine temporal and spatial resolutions. In the absence of information on small-scale dynamical forcing, aerosol composition, and fine structure of supersaturation prior to ice formation, it can be difficult to detect homogeneous freezing layers in observations. The ice nucleation stage by itself may have little predictive power about the morphology of, and distribution of physical variables within, cirrus clouds.

In episodes of strong turbulence, entrainment mixing could affect homogeneous freezing within dynamically active regions. In part due to high levels of turbulence in and around mesoscale convective systems, the warm cirrus regime that includes cloud droplet freezing seems to be especially prone to turbulence effects, but turbulence intensities might at times be large enough to affect homogeneous freezing even in the TTL.

Acknowledgments
This study was conceived and written while B.K. was a CIRES Sabbatical Visiting Fellow at NOAA ESRL. We thank Dan Murphy for discussions and insightful comments and Aurélien Podglajen for valuable feedback on the manuscript. No data were used in producing this manuscript.

References

Diao, M., M. A. Zondlo, A. J. Heymsfield, S. P. Beaton, and D. C. Rogers (2013), Evolution of ice crystal regions on the microscale based on in situ observations, *Geophys. Res. Lett.*, *40*, 3473–3478, doi:10.1002/grl.50665.

Dinh, T., S. Fueglistaler, D. Durran, and T. Ackerman (2014), Cirrus and water vapor transport in the tropical tropopause layer—Part 2: Roles of ice nucelation and sedimentation, cloud dynamics and moisture conditions, *Atmos. Chem. Phys.*, *14*, 12,225–12,236.

Dinh, T., A. Podglajen, A. Hertzog, B. Legras, and R. Plougonven (2016), Effect of gravity wave temperature fluctuations on homogeneous ice nucleation in the tropical tropopause layer, *Atmos. Chem. Phys.*, *16*, 35–46.

Dürbeck, T., and T. Gerz (1996), Dispersion of aircraft exhausts in the free atmosphere, *J. Geophys Res.*, *101*(D20), 26,007–26,015.

Haag, W., B. Kärcher, S. Schaefers, O. Stetzer, O. Möhler, U. Schurath, M. Krämer, and C. Schiller (2003), Numerical simulations of homogeneous freezing processes in the aerosol chamber AIDA, *Atmos. Chem. Phys.*, *3*, 195–210.

Hoyle, C. R., B. P. Luo, and Th. Peter (2005), The origin of high ice crystal number densities in cirrus clouds, *J. Atmos. Sci.*, *62*, 2568–2579.

Kärcher, B. (2003), Simulating gas-aerosol-cirrus interactions: Process-oriented microphysical model and applications, *Atmos. Chem. Phys.*, *3*, 1645–1664.

Kärcher, B. (2017), Cirrus clouds and their response to anthropogenic activities, *Curr. Clim. Change Rep.*, *3*, 1–13, doi:10.1007/s40641-017-0060-3.

Kärcher, B., and U. Lohmann (2002), A parameterization of cirrus cloud formation: Homogeneous freezing of supercooled aerosols, *J. Geophys Res.*, *107*, 4010, doi:10.1029/2001JD000470.

Kärcher, B., and A. Seifert (2016), On homogeneous ice formation in liquid clouds, *Q. J. R. Meteorol. Soc.*, *142*, 1320–1334, doi:10.1002/qj.2735.

Kärcher, B., A. Dörnbrack, and I. Sölch (2014), Supersaturation variability and cirrus ice crystal size distributions, *J. Atmos Sci.*, *71*, 2905–2926.

Jensen, E. J., et al. (2008), Formation of large ($\simeq$100μm) ice crystals near the tropical tropopause, *Atmos. Chem. Phys.*, *8*, 1621–1633.

Jensen, E. J., G. Diskin, R. P. Lawson, S. Lance, T. P. Bui, D. Hlavka, M. McGille, L. Pfister, O. B. Toon, and R. Gao (2013a), Ice nucleation and dehydration in the tropical tropopause layer, *Proc. Natl. Acad. Sci. U.S.A.*, *47*, 2041–2046.

Jensen, E. J., R. P. Lawson, J. W. Bergman, L. Pfister, T. P. Bui, and C. G. Schmitt (2013b), Physical processes controlling ice concentrations in synoptically forced, midlatitude cirrus, *J. Geophys Res.*, *118*, 1–13, doi:10.1002/jgrd.50421.

Jensen, E. J., R. Ueyama, L. Pfister, T. V. Bui, R. P. Lawson, S. Woods, T. Thornberry, and A. W. Rollins (2016a), On the susceptibility of cold tropical cirrus to ice nuclei abundance, *J. Atmos. Sci.*, *73*, 2445–2464.

Jensen, E. J., R. Ueyama, L. Pfister, T. V. Bui, M. J. Alexander, A. Podglajen, A. Hertzog, S. Woods, R. P. Lawson, J.-E. Kim, and M. R. Schoeberl (2016b), High-frequency gravity waves and homogeneous ice nucleation in tropical tropopause layer cirrus, *Geophys. Res. Lett.*, *43*, 6629–6635, doi:10.1002/2016GL069426.

Koop, T., B. P. Luo, A. Tsias, and Th. Peter (2000), Water activity as the determinant for homogeneous ice nucleation in aqueous solutions, *Nature*, *406*, 611–614.

Lane, T. P., and R. D. Sharman (2014), Intensity of thunderstorm-generated turbulence revealed by large-eddy simulation, *Geophys. Res. Lett.*, *41*, 2221–2227, doi:10.1002/2014GL059299.

Li, Q., M. Rapp, A. Schrön, A. Schneider, and G. Stober (2016), Derivation of turbulent energy dissipation rate with MAARSY and radiosondes at Andoya, Norway, *Ann. Geophys.*, *34*, 1209–1229, doi:10.5194/angeo-34-1209-2016.

Lin, R.-F., D. O. Starr, J. Reichardt, and P. J. DeMott (2005), Nucleation in synoptically forced cirrostratus, *J. Geophys Res.*, *110*, D08208, doi:10.1029/2004JD005362.

Murphy, D. M. (2014), Rare temperature histories and cirrus ice number density in a parcel and a one-dimensional model, *Atmos. Chem. Phys.*, *14*, 13,013–13,022.

Murphy, D. M., and T. Koop (2005), Review of the vapour pressures of ice and supercooled water for atmospheric applications, *Q. J. R. Meteorol. Soc.*, *131*, 1539–1565, doi:10.1256/qj.04.94.

Podglajen, A., A. Hertzog, R. Plougonven, and B. Legras (2016), Lagrangian temperature and vertical velocity fluctuations due to gravity waves in the lower stratosphere, *Geophys Res. Lett.*, *43*, 3543–3553, doi:10.1002/2016GL068148.

Riechers, B., F. Wittbracht, A. Hütten, and T. Koop (2013), The homogeneous ice nucleation rate of water droplets produced in a microfluidic device and the role of temperature uncertainty, *Phys. Chem. Chem. Phys.*, *15*, 5873–5887.

Shi, X., and X. Liu (2016), Effect of cloud-scale vertical velocity on the contribution of homogeneous nucleation to cirrus formation and radiative forcing, *Geophys Res. Lett.*, *43*, 6588–6595, doi:10.1002/2016GL069531.